Scientific paper

Preparation and Investigation of the Thermal Stability of Phosphate-modified TiO_2 Anatase Powders and Thin Films

Uroš Prah* and Irena Kozjek Škofic

Faculty of Chemistry and Chemical Technology, University of Ljubljana, Večna pot 113, SI-Ljubljana, Slovenia

** Corresponding author: E-mail: prah.uros@gmail.com*

Received: 04-05-2017

Abstract

The temperature dependence of the anatase-to-rutile phase transition of TiO_2 powders and thin films was studied. In order to shift the phase transition to higher temperature, samples were doped with a different amount of phosphate ions and their influence on the structure and thermal stability of the anatase phase was investigated. In addition, the effect of the catalyst form (powders or thin films) on the temperature of the anatase-to-rutile phase transition was observed. TiO_2 thin films and powders were prepared using a simple sol-gel method with an alkoxide precursor and citric acid. The thin films were deposited on silicon and aluminum substrates using the dip-coating technique. The content of the anatase phase and the crystallite size at different annealing temperatures were monitored using X-ray diffraction. The course of the thermal decomposition was followed using thermal analyses. The morphology, particle size, shape and elemental makeup of the samples were investigated using scanning electron microscopy and energy-dispersive X-ray spectroscopy. The results showed that the phosphate ions successfully inhibited the growth of the anatase nanoparticles and delayed the phase transition to the rutile phase.

Keywords: Anatase, phosphate, sol-gel, thermal stability, thin films

1. Introduction

During the past few decades titanium dioxide has been one of the most intensively studied semiconductor materials. It has numerous useful characteristics, such as the unique positions of the valence and conduction bands, a relatively narrow band-gap, chemical and physical stability, favorable electronic and optical properties, non-toxicity and a low price.[1–7] Furthermore, in nanocrystalline form it shows good catalytic and photocatalytic properties. Photons with sufficient energy excite electrons into the conduction band, which leads to the generation of free electrons in the conduction band and positive holes in the valence band. The energy required for the photogeneration of the electron-hole pairs in TiO_2 nanocrystals is 3.0–3.2 eV, which is equivalent to the energy of light in the near-UV region.[8] Some of these pairs react with electron-donor and electron-acceptor species on the semiconductor surface to form reactive radicals, which can be used for the degradation of environmental pollutants, self-cleaning, antifogging and the sterilization of surfaces.[4,5]

TiO_2 naturally occurs in three polymorph crystal modifications: rutile, anatase and brookite.[5,6,9] Of these, the anatase and rutile phases are the most frequently used, while brookite is less interesting for practical applications due to its lower thermal stability and difficult preparation. Although the band-gap of the anatase phase is wider (3.2 eV) in comparison to rutile (3.0 eV), anatase is considered to exhibit better photocatalytic activity due to its larger surface area and the slower recombination process for the charge carriers.[6,10,11] The anatase is thermodynamically metastable and irreversibly converts to rutile at higher temperatures. This phase transition results in a reduction of the photocatalytic activity (formation of the less-active rutile form) and causes undesirable dimensional changes of the material.[12] Improving the thermal stability of the anatase phase, by increasing the temperature of the anatase-to-rutile phase transition, is particularly important when using TiO_2 in high-temperature applications, such as the degradation of toxic NO_x and SO_x, which are usually produced at high temperatures.[13,14]

To achieve a better thermal stability of the anatase phase and thereby inhibit the anatase-to-rutile phase transformation, different ion dopants (F^-, Si^{4+}, Fe^{3+}, Al^{3+}, etc.) were added to pure TiO_2. These dopants can occupy both interstitial and substitutional positions in the TiO_2

crystal lattice or act like a steric barrier (form a layer on the particles' surface) and thus shift the phase transformation to higher temperatures and therefore enhance the thermal stability of the anatase phase.[1,3,6,10,13–16] Phosphate ions react with uncondensed hydroxyl groups on the surface of TiO_2 particles and act as a steric barrier. Thereby phosphate ions effectively hold the anatase particles at certain distance (inhibit the contacts among the particles) and consequently decelerate their growth, because the rutile phase, which is responsible for a drastic increase in the particle size, begins to form at the interface between the anatase particles in the TiO_2 agglomerates.[1,17,18] By keeping the anatase particles separated at a certain distance, the phase transformation can be restricted and at the same time the small particle size can be maintained.[1,3,6,16]

The sol-gel technique is one of the most frequently used methods for the preparation of TiO_2. The particle size and the morphology of the product can be easily controlled by changing the synthesis parameters. The variety of the prepared products, such as thin films, fibers, xerogels, aerogels, powders and dense ceramics, allows very diverse applications. Different types and amounts of dopants or additives can be easily added during the synthesis. A high degree of homogeneity for the prepared materials can be achieved in a single or even in multicomponent systems.[7,19,20]

Using a powdered catalyst is not favorable for heterogeneous photocatalysis. The problem is its mobility in air and removal from aqueous systems. To avoid these problems, powders are often immobilized on various substrates, for example, thin films can be prepared.[4] The advantages of using thin films are their easy removal from the liquid media and the low consumption of raw materials. In addition, very thin and transparent thin films can be prepared and used for different applications, such as self-cleaning windows and anti-fogging mirrors. Thin films often exhibit different properties compared to powders, such as phase composition, microstructure, reactivity, etc. Therefore, apart from the influence of phosphate ion addition, the influence of the TiO_2 catalyst form (powder or thin film) and the impact of immobilization on the course of the phase conversion of anatase into rutile were studied.

2. Experimental

2. 1. Chemicals and Materials

Titanium(IV) butoxide (97%), citric acid (≥ 99.5%) and absolute ethanol (≥ 99.8%) were purchased from Sigma Aldrich. Phosphoric acid (85%) was procured from Alfa Aesar. All chemicals were used without further purification. Aluminum foil (thickness 0.01 mm) and pure silicon wafers (1-0-0 single crystal, prepared by Czochralski method, MEMC Elect. Materials Sdn. Bhd.) were used as the substrates for the thin films.

2. 2. Synthesis

Sols of TiO_2 and TiO_2 doped with phosphate ions were prepared by dissolving 0.01 mol of citric acid in 20 mL of absolute ethanol. The mixture was stirred on a magnetic stirrer until all the acid was dissolved and then 0.01 mol of titanium butoxide was slowly added to the solution. The beaker with the colloidal solution was closed with parafilm and the stirring was continued for approximately 12 hours. All the sols were stored in a refrigerator (5 °C) until further use.

For the doped sols, the only difference was the addition of a different quantity of phosphoric acid to the homogenous solution of citric acid in ethanol before the addition of the Ti-precursor. Relative to the titanium ions, 5 mol%, 10 mol% and 15 mol% of phosphate ions were added to the solutions.

2. 3. Preparation of Powders and Thin Films

For the preparation of the powders, the sols were dried in air at room temperature to produce the xerogels. The films were deposited using the dip-coating technique on aluminum foil and silicon plates, which were first cut to appropriate dimensions and cleaned in an ultrasonic bath in deionized water, followed by absolute ethanol, and then dried. The film thicknesses and their homogeneities were controlled using a constant pulling velocity (20 cm min^{-1}). The thin films were dried in air at room temperature. The thin films had good adhesive properties (layers could not be removed by rubbing and cutting) and therefore no additional surfactant was needed. All the prepared xerogels and the dried thin films were then calcined for 1 hour at 400, 500, 600, 700, 800, 900 and 1000 °C. After the calcinations, the powders were thoroughly milled in an agate mortar.

2. 4. Characterization

The thermal analyses of the xerogels and thin films were carried out in a dynamic air atmosphere with a flow rate of 100 mL min^{-1} on a Mettler Toledo TGA/DSC 1 thermo analyzer, coupled with a Balzers Thermostar quadrupole mass spectrometer. Aluminum foil was used as the supporting material for the thin films. The thin films were cut into small pieces (~2 mm x 2 mm) and analyzed in the temperature range from room temperature up to 600 °C, while the xerogels were measured up to 800 °C. For all the measurements 150-μL platinum crucibles were used. Firstly, the samples were purged with air at 25 °C for 20 min and then heated at 5 K min^{-1}. The gas products were transferred to the mass spectrometer through the quartz capillary heated to 190 °C. The baseline was subtracted for all the samples.

The X-ray diffraction (XRD) patterns were recorded on an X PANalytical X`Pert PRO diffractometer using monochromatic Cu-Kα radiation. Measurements of the

heat-treated powders were recorded from 2θ = 15° to 60° with a step of 0.034 degrees per second and an integration time of 100 s. Thin films were recorded from 2θ = 23° to 30° with a step of 0.034 degrees per second and an integration time of 500 s. For the XRD analysis, silicon plates were used as a support for the thin films since silicon does not have any peaks in the 2θ measuring range.

Scanning electron microscope (SEM) images of the samples were taken with a Zeiss Ultra Plus field-emission scanning electron microscope. A small amount of powders and appropriately cut thin films on silicon plates (~5 mm × 5 mm) were attached to carbon tape on the metal holders. The electrical conductivity of titanium dioxide is sufficient; therefore, sputtering with conductive material was not needed.

The elemental composition and the distribution of the elements in the samples were determined using energy-dispersive X-ray spectroscopy (EDS) coupled to SEM.

3. Results and Discussion

3. 1. Thermal Analysis

The thermal decomposition of the xerogels and the thin films was investigated using thermal analysis. The mass losses, exothermic and endothermic changes of the samples during the thermal treatment were measured with thermogravimetric analysis (TG) and differential scanning calorimetry (DSC). For a qualitative analysis of the released gases and for better understanding of the thermal decomposition, mass spectrometry (MS) was also employed. DSC analysis was used to determine the temperature where the anatase-to-rutile phase transition took place. This phenomenon is very hard to detect for at least two reasons. One reason is a very small exothermic effect that accompanies this phase transformation and the other is its position, which is highly dependent on the selected synthesis method and the experimental parameters.[21]

Fig. 1 shows the results of the thermal decomposition of the undoped xerogel sample. Three distinct steps of mass loss were observed. In the first step between room temperature and 150 °C, the weight loss was 7.5%, corresponding to water and ethanol evaporation (m/z 18 and 46). Water evaporation also took place at the beginning of the following step of the mass loss, which is evident from the endothermic minimum on the DSC curve. In the second step, from 150 °C to around 370 °C, the mass decreases by approximately 46% and the third step continued up to 530 °C, with a mass loss of approximately 18%. The last two steps of the mass loss are associated with the decomposition and oxidation of the organic compounds (residues of the citric acid and butoxide groups), which is also supported by the peaks of the alkyl fragments, carbon dioxide and water from the MS signals. The total mass loss of the sample is around 72%. No exothermic peak that could represent the anatase-to-rutile phase transition is observed.

The thermal decomposition of the doped samples is comparable to the undoped sample (Fig. 2). The first and second steps of the thermal decomposition of all the samples occur in the same temperature range and show almost

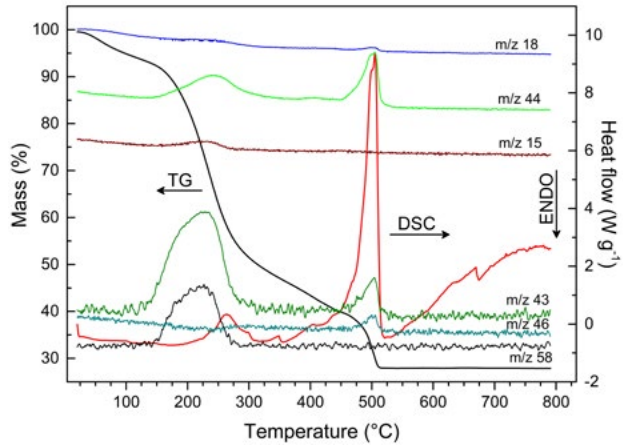

Figure 1. TG, DSC curves and signals from MS of undoped xerogel.

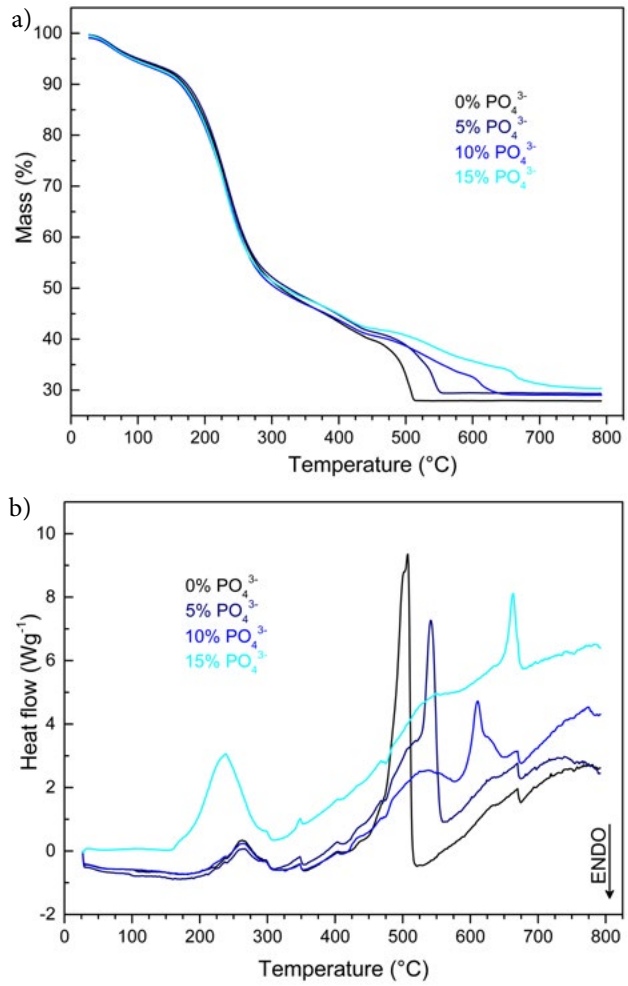

Figure 2. A comparison of (a) TG and (b) DSC curves of doped and undoped xerogels.

identical mass losses, regardless of the quantity of phosphate ions added (overlapping TG curves). The only observed difference is in the last stage of the thermal decomposition, where the temperature of the oxidation of the organic compounds moves to higher temperatures with an increasing amount of added dopant. Therefore, the mass is stabilized at higher values, which have an impact on the selection of the lowest annealing temperature. The same observations were made in the comparison of the DSC curves, wherein the addition of phosphate ions moved the exothermic peak of the last stage of thermal decomposition to higher temperatures, where also instead of one exothermic peak, two smaller one were observed.

Thermal analyses of the thin films deposited on the aluminium foil were also investigated. Due to the much heavier aluminium substrate in comparison to the thin layer, all the effects were much harder to detect. Weight changes during the thermal treatment and also exothermic and endothermic effects were very low and their interpretation was easier in comparison to the results of the xerogels (Fig. 3).[22,23] The total mass loss in the thin films was around 3.5%. However, it should be taken into consideration that the thermal decomposition of the thin films is often carried out differently than in the case of xerogels, because of the suppressed diffusion of gases on the substrate side, the decomposition steps are not so clear.[24] Despite this difference, the positions of the more intense exothermic and endothermic peaks and the temperature of the total mass loss are positioned in the same temperature ranges.

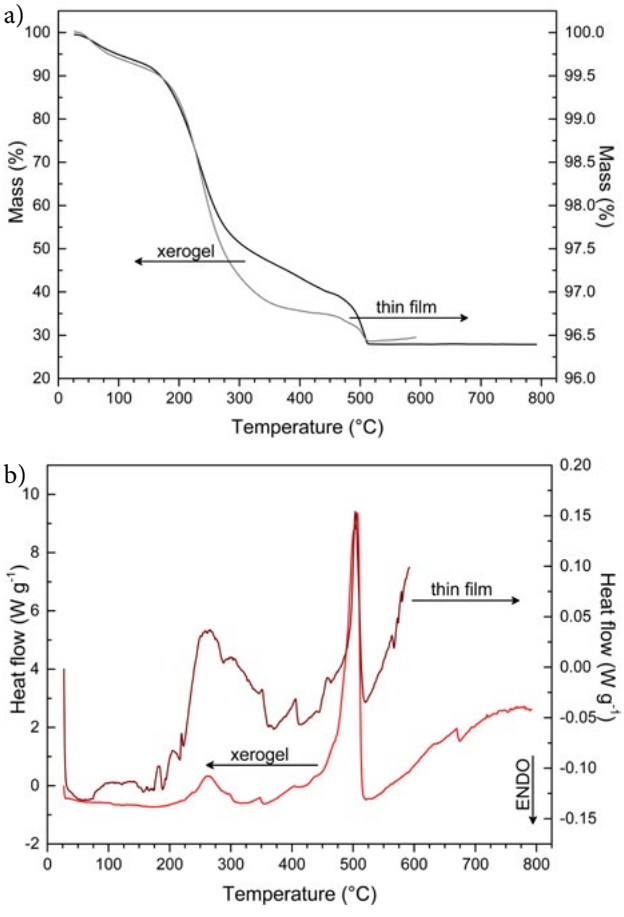

Figure 3. A comparison of (a) TG and (b) DSC curves for the undoped xerogel and the thin film.

Based on the results of the thermal analysis, a range of annealing temperatures was selected. Because we could not determine the exact temperature where the anatase-to-rutile phase transition occurred, we used a wider range of annealing temperatures. The used temperatures were 400, 500, 600, 700, 800, 900 and 1000 °C.

3. 2. XRD Analysis

The content of the anatase phase and the particle size were determined by XRD analysis and calculated using the Rietveld analysis and Scherrer formula. The results were calculated from all the peaks in the measuring range and not only from the peaks 2θ = 25.28° (101) and 27.40° (110), which are often taken as the characteristic peaks of the anatase and rutile phases.[1,25,26]

Firstly, the influence of adding phosphate ions on the average particle size and the thermal stability of the anatase phase in the powders were monitored (Fig. 4). In the undoped samples, the content of the anatase phase quickly dropped with an increasing annealing temperature. At 400 °C amorphous and partially crystallized anatase phase was present, but the content of the anatase phase dropped rapidly to 6.4 wt%, when it was annealed at 600 °C. The particle size increased with the increasing temperature and it was 30 nm at 600 °C (Table 1). When the anatase particles are sufficiently large, they start to interact with each other and the phase transformation occurs at the interfaces between them. With an increasing annealing temperature, more anatase particles were converted to rutile and the phase transformation gradually extends over the entire TiO_2 agglomerates.

In doped TiO_2, the phosphate ions can easily react with the surface hydroxyl groups and form a layer on the surfaces of the anatase nanoparticles. The phosphates act like a steric barrier that prevents any direct contact between the particles, inhibits their growth and the interactions among them. By inhibiting the particle growth and preventing any interaction between the particles, the phase transformation occurs at higher temperatures.[1] The doped powders (with 5, 10 and 15 mol%) showed better thermal stability for the anatase with an increasing proportion of added dopant. The best results were shown by the sample with 15 mol% of added dopant, where only the anatase phase was present up to 700 °C. At 800 °C the anatase content decreased to 74.7% and at 900 °C to 6.8%. At higher dopant ratios (10 and 15 mol%) and high annealing temperatures (900 and 1000 °C) the formation of the new crystal phase, titanyl phosphate, was observed (3–10 wt%), otherwise only the anatase and rutile phases were present (Fig. 5b). All the samples annealed at 1000 °C contained, besides titanyl phosphate, only the rutile phase. The phos-

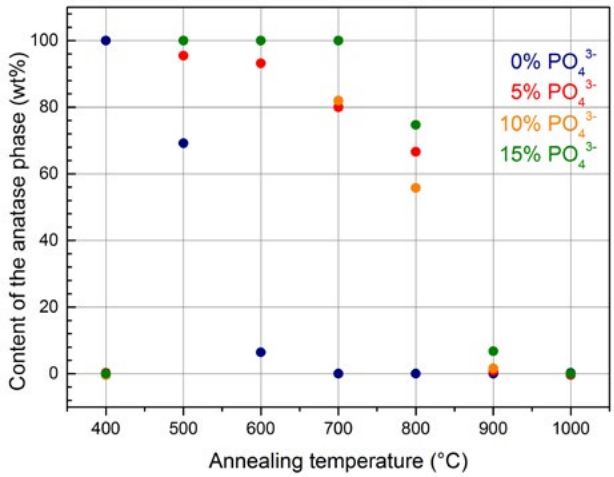

Figure 4. Content of anatase phase depending on the dopant ratio at different annealing temperatures in the powders.

Table 1. Average size of the anatase particles in powders with different annealing temperatures and dopant ratios.

Annealing temperature (°C)	Dopant ratio (mol%) 0	5	10	15
	Average size of the anatase particles (nm)			
400	~8[c]	0[a]	0[a]	0[a]
500	16.6	~7[c]	~6[c]	~10[c]
600	30.0	8.4	6.6	6.0
700	0[b]	11.7	8.1	7.8
800	0[b]	22.9	25.9	28.7
900	0[b]	26.4	38.8	43.6
1000	0[b]	0[b]	0[b]	0[b]

a – amorphous phase b – all anatase has been converted to rutile
c – estimated value based on a partially crystallized anatase

phate ions improved the thermal stability of the anatase phase and raised the temperature of the present anatase

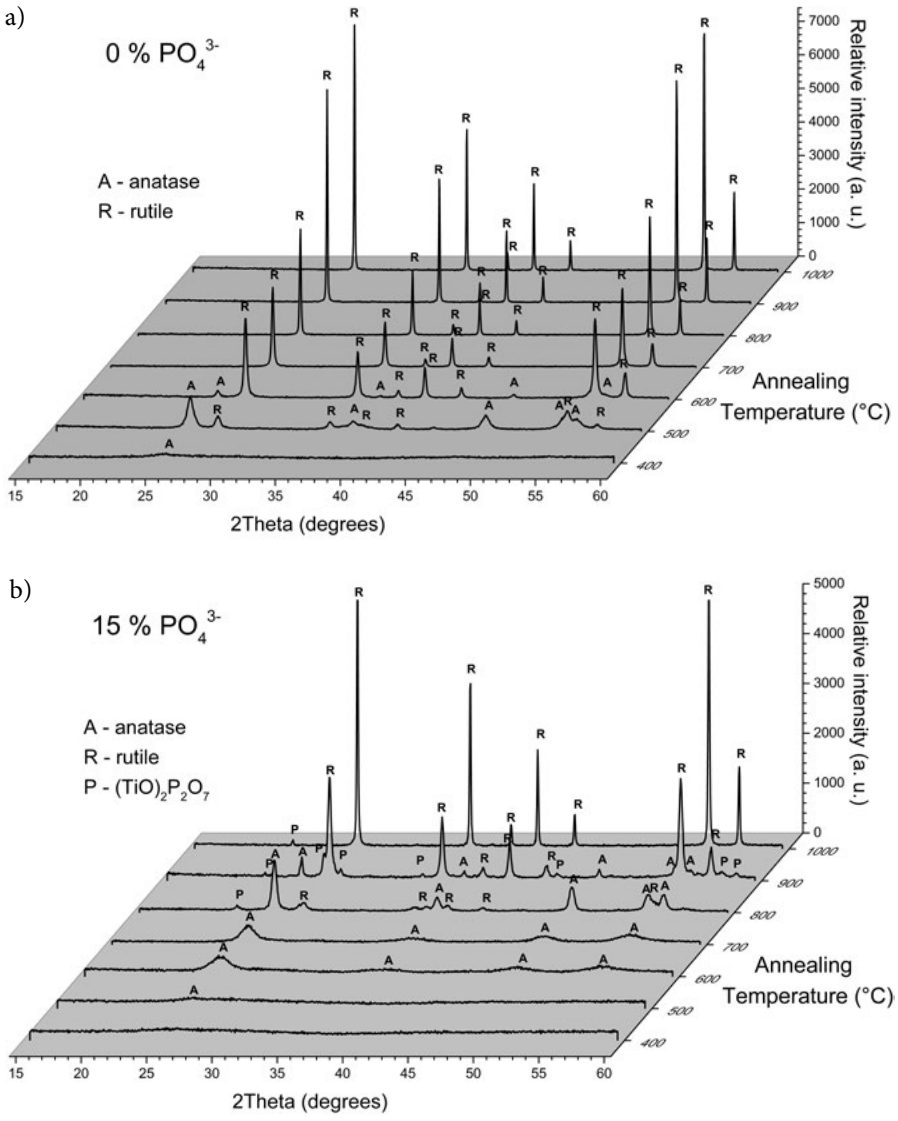

Figure 5. Evolution of the recorded powder diffraction patterns with an increasing annealing temperature (a: undoped TiO_2 nanoparticles, b: TiO_2 nanoparticles doped with 15 mol% of phosphate ions).

phase to 900 °C. The average size of the anatase particles was successfully inhibited by the phosphate ions up to 700 °C, where the average particles size remained under 12 nm (Table 1). At temperatures above 800 °C, the steric barrier is no longer able to prevent the particle growth and the phase transformation starts to take place. On the other hand, the addition of phosphate ions also increased the crystallization temperature of the anatase phase, because in doped samples, annealed at temperatures below 500 °C, no crystalline phase was observed (Table 1).

The formation of all the crystalline phases and the particle growth are clear from the series of diffractograms (Fig. 5) that were recorded after the heat treatment at different temperatures for the undoped and (15 mol%) doped powder samples. In the undoped sample, in comparison to the doped sample, the anatase peaks are narrower and have a greater intensity, which is indicative of a larger particle size.

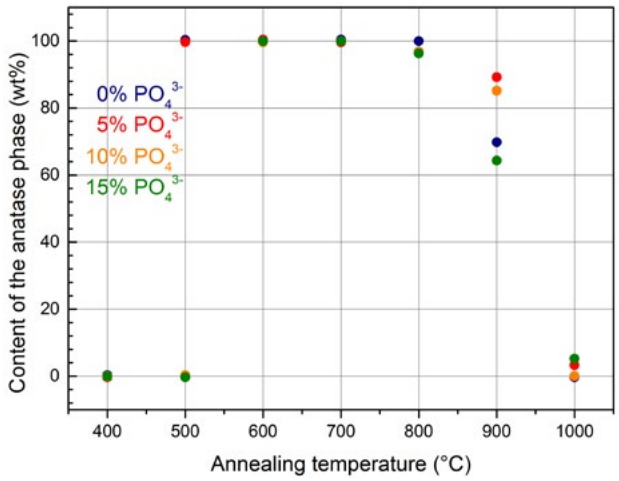

Figure 6. Dependence of the amount of anatase phase on the dopant ratio for different annealing temperatures in thin films.

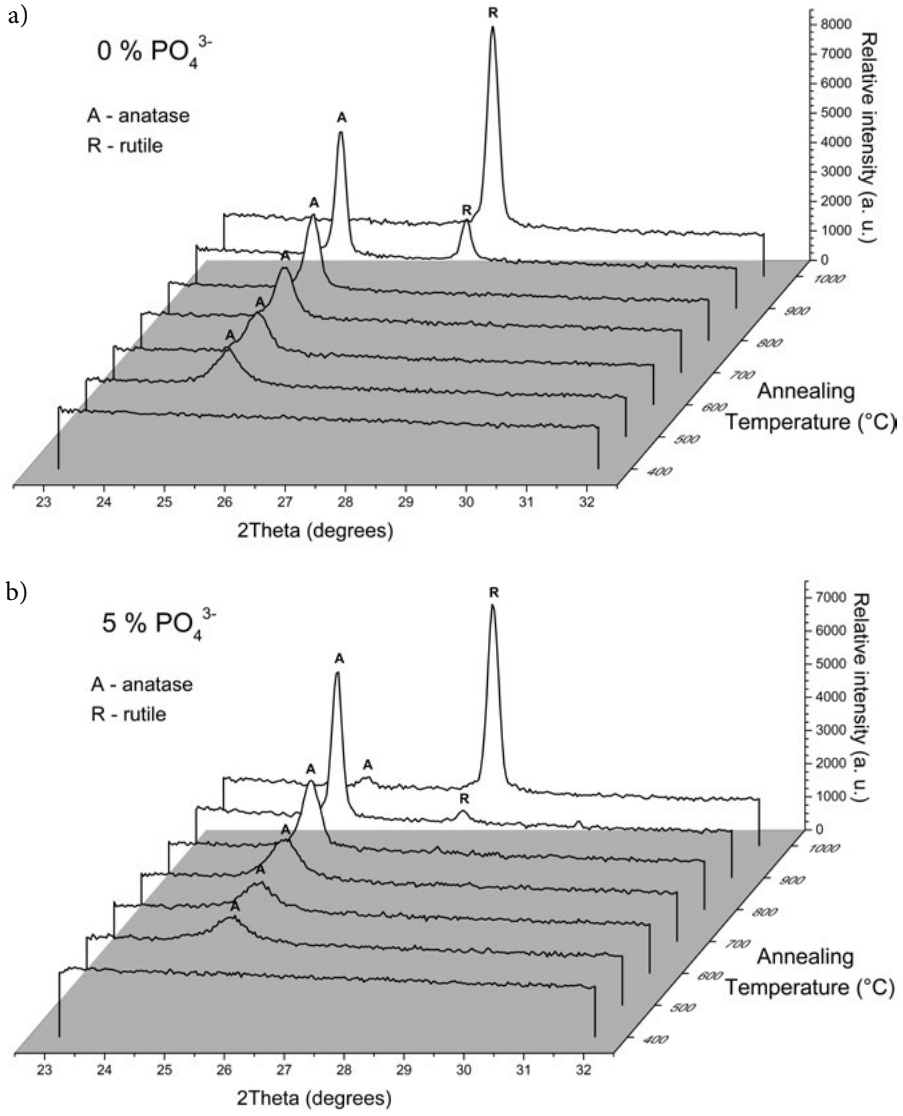

Figure 7. Evolution of the recorded diffraction patterns with an increasing annealing temperature (a: undoped TiO_2 thin films, b: TiO_2 thin films doped with 5 mol% of phosphate ions).

Table 2. Average size of the anatase particles in thin films with different annealing temperatures and dopant ratios.

Annealing temperature (°C)	Dopant ratio (mol%) 0	5	10	15
	Average size of the anatase particles (nm)			
400	0[a]	0[a]	0[a]	0[a]
500	18.2	13.7	0[a]	0[a]
600	21.6	14.5	9.1	10.7
700	27.7	15.1	8.6	8.6
800	38.3	29.4	29.0	17.0
900	58.6	58.4	64.1	65.2
1000	0[b]	53.3	0[b]	52.4

a – amorphous phase b – all anatase has been converted to rutile

The influence of phosphate ions on the anatase's thermal stability in thin films is illustrated in Fig. 6. In thin films, compared to powders, a much smaller difference between the doped and the undoped samples was detected. In the undoped sample, even at 800 °C, only the anatase phase was present. At higher temperatures, the content of the anatase phase dropped rapidly and at 900 °C it was approximately 70 wt%. At 1000 °C only the rutile phase was detected. The thermal stability of the anatase phase was slightly improved by adding phosphate ions. The best results were shown by the sample with 5 mol% dopant, where at 900 °C there was approximately 90 wt% of anatase phase. Even at 1000 °C, approximately 5 wt% of anatase phase was detected. In all the samples and at all the annealing temperatures only the anatase and rutile phases were present and no titanyl phosphate was formed. In thin films doped with 5 mol% of phosphate ions, the anatase phase was already crystallized at 500 °C, but in samples with higher content of the added dopant (10 and 15 mol%) the temperature of the anatase crystallization increased to 600 °C.

The reason why the anatase phase in the undoped thin films is more stable than in the powders is in the thickness of the thin films. In thin films, there is a limited amount of TiO_2 because the layer is very thin and is blocked by the substrate on one side. Such a thin layer does not provide enough material for the growth of the anatase particles (Table 2) and the transformation to rutile phase. The formation of the anatase and rutile phases and their particle growth is evidenced by the series of diffractograms of the thin films on silicon (Fig. 7), which were recorded after annealing at different temperatures. In addition, the difference between the undoped sample and the sample doped with 5 mol% of phosphate ions was apparent.

3. 3. SEM Analysis

To study the morphology, particle shape and size, SEM images of all the prepared thin films and powders were taken. The nanoparticles in the powders were not iso-

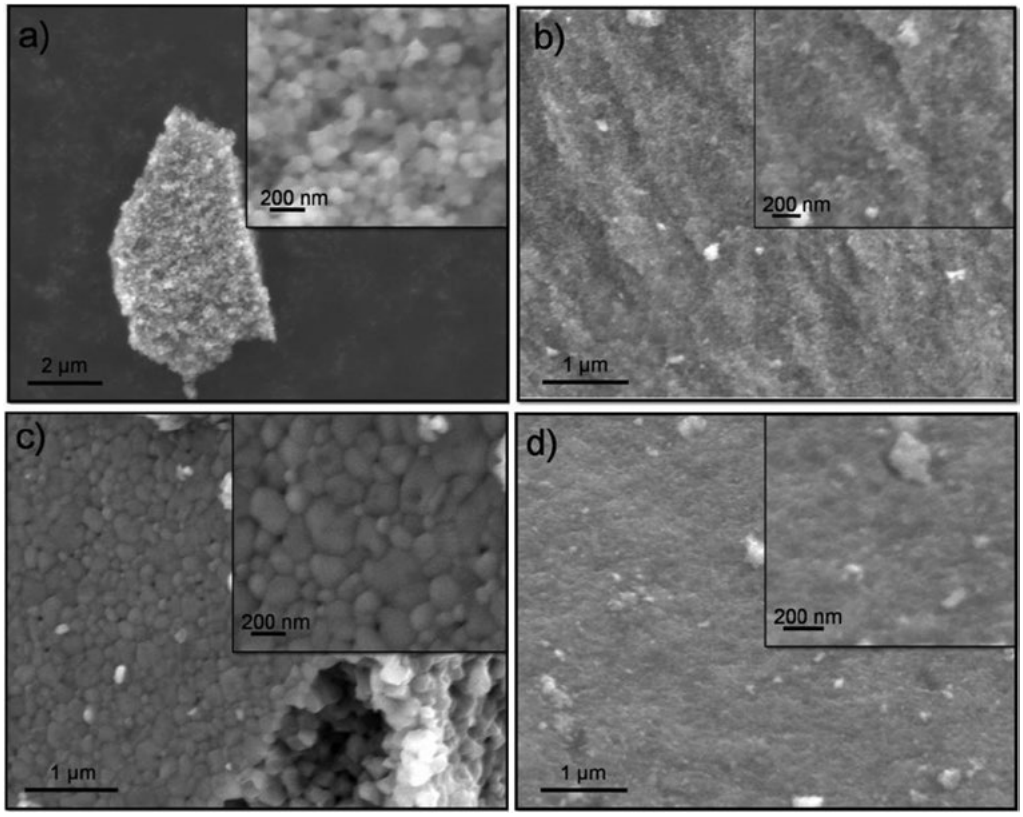

Figure 8. SEM micrographs of powders: a) 0% PO_4^{3-}, 800 °C b) 15% PO_4^{3-}, 800 °C c) 5% PO_4^{3-}, 1000 °C and d) 5% PO_4^{3-}, 500 °C.

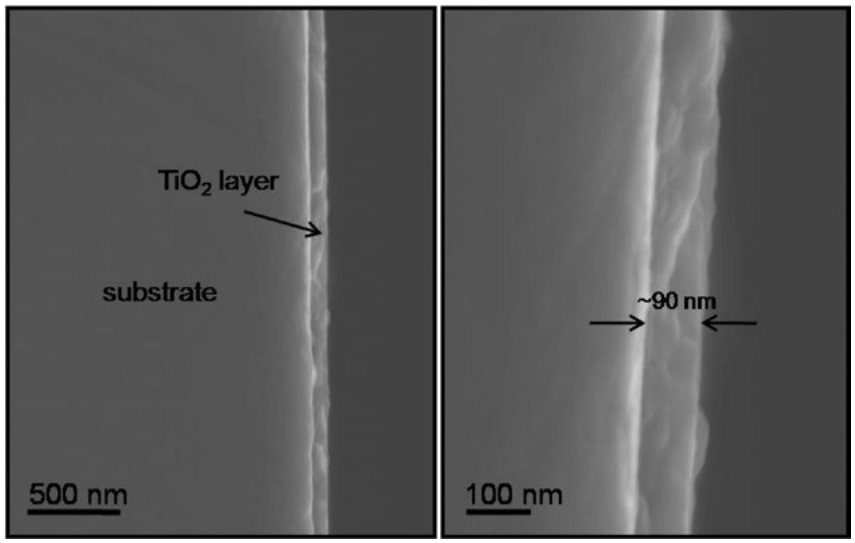

Figure 9. SEM micrographs of a cross-section of undoped thin film, calcined at 600 °C.

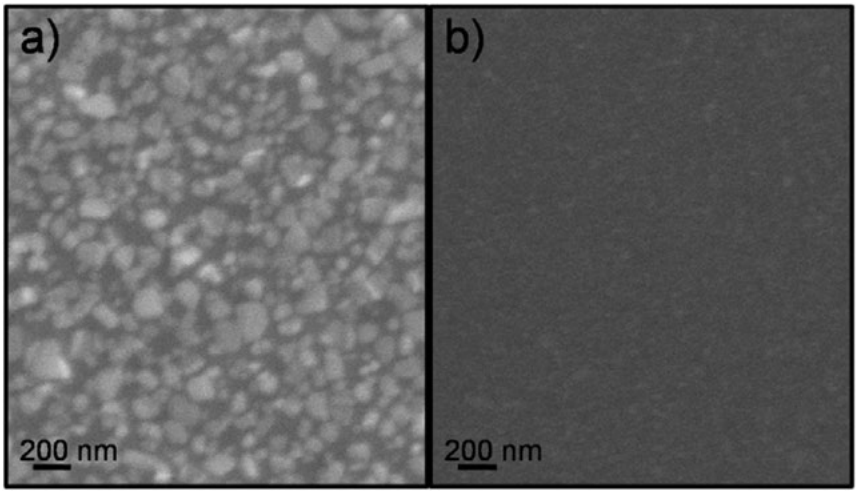

Figure 10. SEM micrographs of thin films: a) 0% PO_4^{3-}, 1000 °C and b) 0% PO_4^{3-}, 600 °C.

lated, but large agglomerates of several micrometers in size and various shapes were formed. The SEM micrograph in Fig. 8 shows that the phosphate ions strongly inhibited the particle growth. At the same annealing temperature, the average particle size decreased with an increasing amount of dopant. The particle size in the undoped samples increased rapidly with the temperature and at 1000 °C, the particles were larger than 100 nm (Fig. 8c and 8d).

In the thin films, uniformly distributed and homogenous layer of about 90 nm thickness were observed (Fig. 9). Even though the thin films were prepared by deposition of only one layer, the films covered the whole substrate equally and no areas without thin film were observed. Due to the limited amount of material in the thin films and the presence of a substrate on one side, smaller average particle size in comparison to the powders was observed (Fig. 10).

3. 4. EDS Analysis

The elemental makeup of the powders and thin films was investigated with EDS analyses. In the doped samples, the larger areas were mapped to evaluate the homogeneity of the phosphorous distribution. With point analyses the molar ratios between the titanium and the phosphorous were measured (Table 3). The results of the mapping analyses (Fig. 11 and 12) showed a uniform distribution of the elements Ti, O and P on the examined surface of the powders and thin films. In the powders, the quantity of measured dopant varied greatly around the value of the initially added amount during the synthesis. These values were strongly dependent on the size and shape of the agglomerates. For example, the proportion of the measured dopant is higher in the case of smaller agglomerates and non-homogeneous surfaces, and smaller in the case of larger ag-

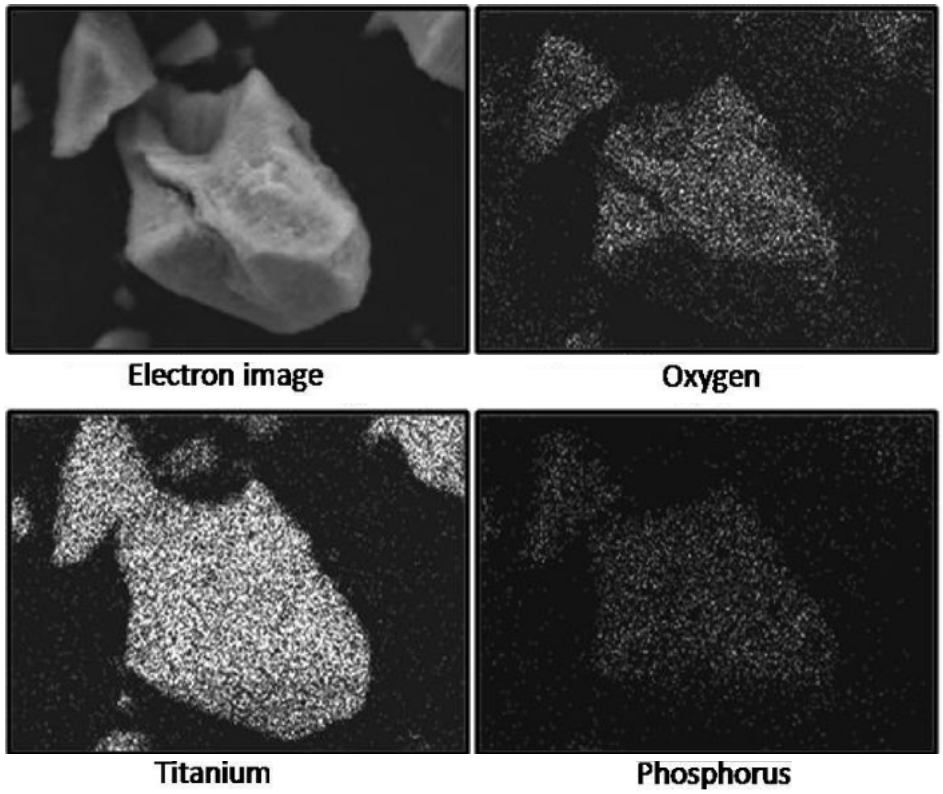

Figure 11. Distribution of the elements Ti, O and P in powder doped with 10 mol% and annealed at 900 °C.

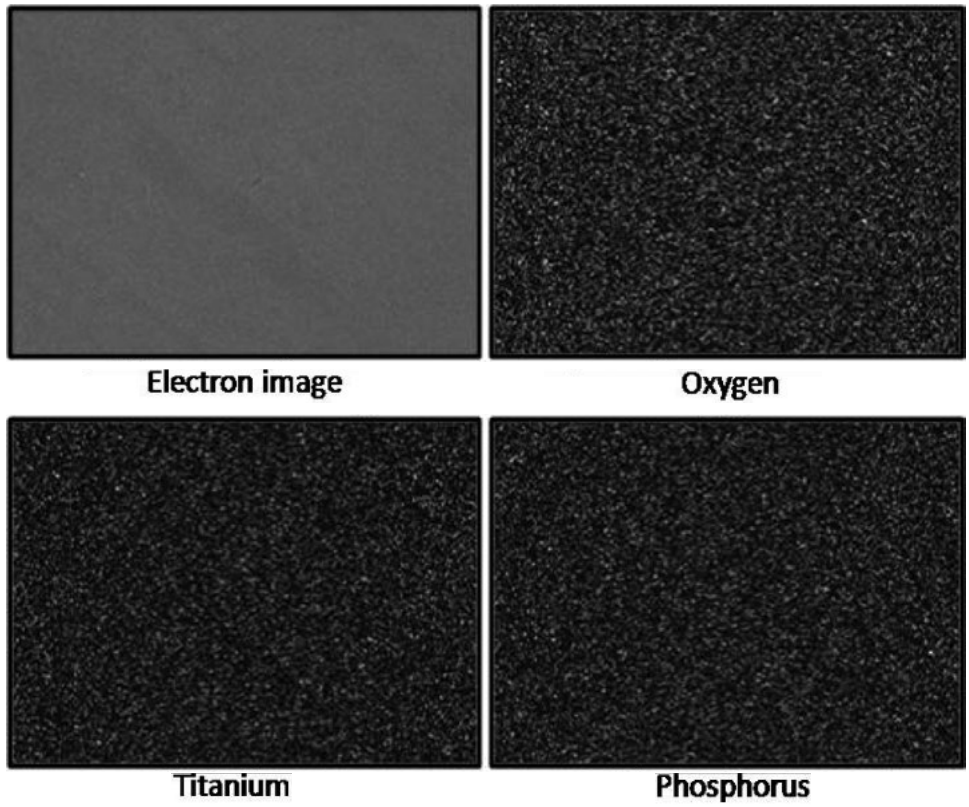

Figure 12. Distribution of the elements Ti, O and P in thin film doped with 15 mol% and annealed at 600 °C.

Table 3. The proportion of added and measured dopant in doped TiO_2 powders and thin films.

Form of the samples	The amount of added dopant (mol%)	The amount of measured dopant (mol%)
Powders	5	4.6
	5	4.7
	5	6.2
	10	10.3
	10	11.0
	10	11.8
Thin films	5	20.4
	5	20.6
	5	21.2
	10	33.3
	10	33.7
	10	34.2
	15	44.1
	15	44.8
	15	45.2

glomerates. Because EDS is a surface technique, this indicates that phosphate ions are mostly distributed on the surface of the particles. In thin films, the amount of measured dopant was much higher than in powders, which is most likely a consequence of a small thickness of the layer.

4. Conclusion

TiO_2 nanopowders and thin films were prepared by a simple and quick sol-gel method using titanium butoxide as the precursor. The samples were doped with phosphate ions and their influence on the thermal stability of the anatase phase was investigated. Increasing the content of added dopant influenced the last stage of the thermal decomposition, which was shifted to higher temperatures and also impacted on the anatase crystallization temperature. The addition of phosphate ions successfully inhibited the anatase-to-rutile phase transition. In the powders, the temperature of the stable anatase phase rose from 600 °C to 900 °C. On the surface of the nanoparticles, the phosphate ions acted as a steric barrier and inhibited the particle interaction and growth, which shifted the phase transition to higher temperatures. In the undoped thin films, the anatase phase showed a good thermal stability, where at 900 °C there was still around 70 wt% of anatase phase. The addition of the phosphate ions improved the thermal stability of the anatase, and even at 1000 °C some amount of anatase phase was observed. The reasons for such different behaviors of the nanopowders and thin films could be the limited amount of material in the thin layer, which does not provide enough material for the particle growth and phase transformation of the anatase to rutile. The surfaces of all the thin films were homogenous, with uniformly distributed layers and in the powders, larger agglomerates were formed. The EDS analysis proved that phosphate ions were mainly bound to the particle surface.

5. References

1. L. Jing, X. Qin, Y. Luan, Y. Qu, M. Xie, *Appl. Surf. Sci.* **2012**, *258*, 3340–3349.
2. M. R. Hoffmann, S. T. Martin, W. Choi, D. W. Bahnemann, *Chem. Rev.* **1995**, *95*, 69–96. **DOI:**10.1021/cr00033a004
3. L. Korösi, I. Dekany, *Colloids Surf. A: Physicochem. Eng. Asp.* **2006**, *280*, 146–154.
4. J. Kumar, A. Bansal, *Water Air Soil Pollut*. **2013**, *224*, 1–11.
5. D. P. Macwan, P. N. Dave, S. Chaturvedi, *J. Mater. Sci.* **2011**, *46*, 3669–3686.
6. K. Elghniji, J. Soro, S. Rossignol, M. Ksibi, *J. Taiwan Inst. Chem. Eng.* **2012**, *43*, 132–139.
7. A. Khataee, G. A. Mansoori: Nanostructured Titanium Dioxide Materials. Properties, Preparation and Applications, World Scientific Publishing Co. Pte. Ltd., Singapore, **2012**, pp. 1–97.
8. A. Fujishima, T. N. Rao, D. A. Tryk, *J. Photochem. Photobiol. C: Photochem. Rev.* **2000**, *1*, 1–21.
9. X. Nie, S. Zhuo, G. Maeng, K. Sohlberg, *Int. J. Photoenergy.* **2009**, 1–22. **DOI:**10.1155/2009/294042
10. D. A. Hanaor, M. H. N. Assadi, S. Li, A. Yu, C. C. Sorrell, *Comput. Mech.* **2012**, *50*, 185 v194.
11. D. A. H. Hanaor, C. C. Sorrell, *J. Mater. Sci.* **2011**, *46*, 855–874.
12. I. Hagarova, P. Matuš, M. Bujdoš, J. Kubova, *Acta Chim. Slov.* **2012**, *59*, 102–108.
13. J. Chen, Q. Shunchen, Z. Yuexiang, X. Youchang, *Chinese J. Catal.* **2011**, *32*, 1173–1179. **DOI:**10.1016/S1872-2067(10)60229-X
14. S. Albonetti, S. Blasioli, M. Bugani, C. Lehaut-Burnouf, S. Augustine, E. Roncari, F. Trifiro, *Environ. Chem. Lett.* **2003**, *1*, 197–200. **DOI:**10.1007/s10311-003-0036-5
15. T. A. Sedneva, E. P. Lokshin, A. T. Belyaevskii, T. Kalinnkov, *Inorg. Mater.* **2008**, *44*, 726–732. **DOI:**10.1134/S0020168508070091
16. V. Žunič, S. D. Škapin, M. Maček Kržmanc, I. Bračko, A. Sever Škapin, D. Suvorov, *Appl. Catal. A: General*. **2011**, *397*, 241–249.
17. J. Zhang, M. J. Li, Z. C. Feng, J. Chen, C. Li, *J. Phys. Chem. B.* **2006**, *110*, 927–935. **DOI:**10.1021/jp0552473
18. D. J. Reidy, D. J. Holmes, M. A. Morris, *Ceram. Int.* **2006**, *32*, 235–239. **DOI:**10.1016/j.ceramint.2005.02.009
19. U. Schubert, N. Hüsing, Synthesis of Inorganic Materials, WILEY-VCH Verlag GmbH & Co. KGaA, Weinheim, **2012**, pp. 155–210.
20. J. Schneider, M. Matsuoka, M. Takeuchi, J. Zhang, Y. Horiuchi, M. Anpo, D. W. Bahnemann, *Chem. Rev.* **2014**, *114*, 9919–9986.
21. A. Dassler, A. Feltz, J. Jung, W. Ludwig, E. Kaisersberg, *J. Therm. Anal.* **1988**, *33*, 803–809. **DOI:**10.1007/BF02138591
22. R. Cerc Korošec, P. Bukovec, B. Pihlar, J. Padežnik Gomilšek,

Thermochim. Acta. **2003**, *402*, 57–67.
DOI:10.1016/S0040-6031(02)00537-3
23. R. Cerc Korošec, P. Bukovec, in: P. R. Somani (Ed): Chromic materials, phenomena and their technological applications. Multifunctional materials and devices, Applied Science Innovations Pvt. Ltd., Pune, India, **2010**, pp. 241–282.
24. R. Cerc Korošec, I. Kozjek Škofic, N. Bukovec, *Thermochim. Acta*, **2004**, 2, 211–217. **DOI:**10.1016/j.tca.2003.08.016
25. L. Q. Jing, B. F. Xin, F. L. Yuan, L. P. Xue, B. Q. Wang, *J. Phys. Chem. B.* **2006**, *110*, 17860–17865.
DOI:10.1021/jp063148z
26. L. Q. Jing, H. G. Fu,B. Q. Wang, D. J. Wang, B. F. Xin, S. D. Li, J. Z. Sun, *Appl. Catal. B.* **2006**, *62*, 282–291.
DOI:10.1016/j.apcatb.2005.08.012

Povzetek

Prahove in tanke plasti TiO_2 smo pripravili po sol-gel sintezni metodi, kjer smo kot prekurzor uporabili titanov butoksid, ki smo mu dodali citronsko kislino. Tanke plasti smo s tehniko potapljanja nanesli na silicijeve in aluminijaste podlage. Plasti in prahove smo dopirali s fosfatnimi ioni ter proučevali njihov vpliv na termično stabilnost anatasne faze. Tanke plasti v primerjavi z nanodelci pogosto prikazujejo različne lastnosti, zato smo analizirali tudi kako oblika pripravljenega vzorca vpliva na fazni prehod anatas-rutil. Odvisnost vsebnosti anatasne faze in velikost kristalitov v odvisnosti od temperature termične obdelave smo spremljali z rentgensko praškovno difrakcijo. Potek termičnega razpada smo analizirali s termično analizo. Z vrstičnim elektronskim mikroskopom smo proučevali obliko, velikost delcev in morfologijo pripravljenih tankih plasti ter s pomočjo energijsko disperzijske spektroskopije tudi njihovo elementno sestavo. Rezultati prikazujejo, da fosfatni ioni uspešno zavirajo rast delcev ter s tem posledično pomaknejo fazni prehod anatas-rutil k višjim temperaturam.